 CMES, vol.6, no.5, pp.477-489, 2004

Meshless Local Petrov-Galerkin Method in Anisotropic Elasticity

J. Sladek[1], **V. Sladek**[1], **S.N. Atluri**[2]

Abstract: A meshless method based on the local Petrov-Galerkin approach is proposed for solution of static and elastodynamic problems in a homogeneous anisotropic medium. The Heaviside step function is used as the test functions in the local weak form. It is leading to derive local boundary integral equations (LBIEs). For transient elastodynamic problems the Laplace transfor technique is applied and the LBIEs are given in the Laplace transform domain. The analyzed domain is covered by small subdomains with a simple geometry such as circles in 2-d problems. The final form of local integral equations has a pure contour character only in elastostatics. In elastodynamics an additional domain integral is involved due to inertia terms. The moving least square (MLS) method is used for approximation of physical quantities in LBIEs.

keyword: meshless method, local weak form, Heaviside step function, moving least squares interpolation, Laplace transform

1 Introduction

A lot of new advanced composite materials used for light and strength structures have anisotropic properties. They are mostly utilized in aerospace structures. It put a requirement to have a reliable and accurate computational method to solve boundary value problems in anisotropic solids. Conventional computational methods with domain (FEM) or boundary (BEM) discretizations have their own drawbacks to solve such kind of problems. It is efficient to apply the conventional boundary element method (BEM) mainly to problems where the fundamental solution is available. The anisotropy increases the number of elastic constants in Hooke's law, hence the construction of fundamental solutions become difficult. In 2-d elastostatic problems the fundamental solution is available in a closed form [Eshelby et al. (1953); Schclar (1994)] and it is given in a complex variable space. Several numerical analyses have been applied to 2-d elastostatic problems [Cruse and Swedlow (1971)] and in specific problems like half-plane [Dumir and Mehta (1987); Pan et al. (1998)], fracture mechanics [Snyder and Cruse (1975); Clements and Haselgrove (1983); Sollero and Aliabadi (1993), (1995); Pan and Amadei (1996); Ang and Telles (2004)] and piezoelectric solids [Pan (1999)]. Closed form fundamental solutions for 3-d anisotropic elasticity exist only for special cases like transversally isotropic or cubic media [Ding et al. (1997)].

Various BEM formulations have been successfully applied to transient elastodynamic problems in isotropic bodies. As regards the time variable treatment one can distinguish three main approaches including the Laplace or Fourier transform formulations [Manolis and Beskos (1988); Dominguez (1993); Sladek and Sladek (1984)], time integration formulation [Cole et al. (1978); Shanz and Antes (1997)], and the mass matrix formulation with domain approximation of inertia terms [Nardini and Brebbia (1983); Perez-Gavilan and Aliabadi (2000)]. In time integration BEM formulation, spatial as well as temporal discretization is required. The fundamental solutions in such a case is quite complicated. It prolongs computational time for evaluation of integrals. In the Laplace transform BEM approach, the fundamental solution is also complex and several quasi-static boundary value problems are to be solved for various values of the Laplace transform parameters. In the mass matrix formulation, one uses the static fundamental solution which is rather simple. However, it leads to boundary-domain integral formulation, because the static fundamental solution is not the solution of the elastodynamic governing equation. Although the domain integral of inertia terms can be converted into boundary integrals by the dual reciprocity method, some additional interior nodes to the boundary ones are required for better spatial approximation of inertia terms. Despite its vast number of applications to dynamic isotropic problems,

[1] Institute of Construction and Architecture, Slovak Academy of Sciences, 84503 Bratislava, Slovakia

[2] Center of Aerospace Education & Research University of California, 5251 California Ave., Irvine, CA 92612, USA

few works are found for analyzing dynamic anisotropic problems [Wang and Achenbach (1996); Albuquerque et al. (2002a,b); Kogl and Gaul (2000)]. The main drawback of boundary element anisotropic formulations is the absence of well-established fundamental solutions. Most anisotropic fundamental solutions for elastodynamics demand numerical integration [Wang and Achenbach (1996)]. The mass matrix formulation is used by Albuquerque et al. (2002a,b).

In spite of the great success of the finite and boundary element methods as effective numerical tools for the solution of boundary value problems on complex domains, there is still a growing interest in development of new advanced methods. Many meshless formulations are becoming to be popular due to their high adaptivity and a low cost to prepare input data for numerical analysis. A variety of meshless methods has been proposed so far [Belytschko et al. (1994); Atluri and Shen (2002a); Atluri (2004)]. Many of them are derived from a weak-form formulation on global domain [Belytschko et al. (1994)] or a set of local subdomains [Atluri and Shen (2002a,b); Atluri (2004); Sladek et al. (2003a,b); Mikhailov (2002)]. In the global formulation background cells are required for the integration of the weak form. In methods based on local weak-form formulation no cells are required and therefore they are often referred to call as truly meshless methods. If for the geometry of subdomains a simple form is chosen, numerical integrations can be easily carried out over them. The meshless local Petrov-Galerkin (MLPG) method is fundamental base for the derivation of many meshless formulations, since trial and test functions are chosen from different functional spaces. The fundamental solution as the test function is leading to accurate numerical results and it was utilized in former papers for isotropic homogeneous and continuously nonhomogeneous bodies under static [Atluri et al. (2000); Sladek et al. (2000)] and dynamic loads [Sladek et al. (2003a, b)]. However, in an anisotropic elasticity the fundamental solution is complex or unavailable in a closed form. From complex fundamental solution it is very difficult to derive the Green's function which vanishes on the local boundary of circular subdomain. It is inappropriate to utilize such a non-vanishing fundamental solution as the test function in derivation of local boundary integral equations, since both the displacements and tractions are unknown on the boundary of the interior sub-domain.

In this paper, the Heaviside step function is used as the test function. It yields a pure contour integral formulation on local boundaries for anisotropic elastostatics, while in elastodynamics an additional domain integral of inertia terms is involved. The spatial variation of the displacement is approximated by the moving least-square (MLS) scheme. After performing the spatial integrations, one obtains the system ordinary differential equations for certain nodal unknowns. That system is solved numerically by the Houbolt finite difference scheme [Houbolt (1950)] as a time stepping method. Alternatively, the Laplace transform is applied to eliminate the time variable. Then, the local boundary integral equations are derived for Laplace transforms. Several quasi-static boundary value problems have to be solved for various values of the Laplace transform parameter. The Stehfest inversion method is applied to obtain the time-dependent solutions. The integral equations have a very simple nonsingular form. Moreover, both the contour and domain integrations can be easily carried out on circular sub-domains. The boundary conditions on the global boundary are satisfied by collocation of the MLS-approximation expressions for the displacements at boundary nodal points.

To demonstrate the accuracy of the present method more numerical examples with simple and more complex geometry are considered for static and dynamic cases.

2 Equilibrium equations

Let us consider a linear elastodynamic problem in an anisotropic domain Ω bounded by the boundary Γ. The equilibrium equation can be expressed as

$$\sigma_{ij,j}(\mathbf{x},t) - \rho \ddot{u}_i(\mathbf{x},t) = -X_i(\mathbf{x},t) \quad , \tag{1}$$

where $\sigma_{ij}(\mathbf{x},t)$ is the stress tensor, $X_i(\mathbf{x},t)$ is the body force vector, ρ is the mass density and $u_i(\mathbf{x},t)$ the displacement vector and the dots indicate the second time derivative. Comma denotes partial differentiation with respect to the spatial coordinates. An elastostatical problem can be considered formally as a special case of the elastodynamical one, with omitting the acceleration $\ddot{u}_i(\mathbf{x},t)$ in the equilibrium equation (1). Therefore, both cases are analyzed simultaneously.

In the case of elastic material, the relation between stress and strain are given by Hooke's law for an anisotropic

body

$$\sigma_{ij}(\mathbf{x},t) = C_{ijkl}\varepsilon_{kl}(\mathbf{x},t) = C_{ijkl}u_{k,l}(\mathbf{x},t) \quad , \tag{2}$$

where C_{ijkl} is the material tensor which exhibits the symmetries

$$C_{ijkl} = C_{jikl} = C_{klij}.$$

The traction vector $t_i(\mathbf{x},t)$ is related to the displacement vector through Cauchy's formula $t_i = \sigma_{ij}n_j$, which leads to

$$t_i(\mathbf{x},t) = C_{ijkl}u_{k,l}(\mathbf{x},t)n_j(\mathbf{x}) \quad , \tag{3}$$

where n_j denotes a unit outward normal vector.

For a plane stress state of a 2-d anisotropic elastic body, the generalized Hooke's law is frequently written through the second order tensor of material constants [Lekhnitskii (1963)]

$$\begin{bmatrix} \varepsilon_{11} \\ \varepsilon_{22} \\ \gamma_{12} \end{bmatrix} = \begin{bmatrix} \beta_{11} & \beta_{12} & \beta_{16} \\ \beta_{12} & \beta_{22} & \beta_{26} \\ \beta_{16} & \beta_{26} & \beta_{66} \end{bmatrix} \begin{bmatrix} \sigma_{11} \\ \sigma_{22} \\ \sigma_{12} \end{bmatrix} , \tag{4}$$

where β_{ij} are the elastic compliances of the material. In the case of plane strain conditions, the coefficients β_{ij} should be replaced by $\tilde{\beta}_{ij}$, where

$$\tilde{\beta}_{ij} = \beta_{ij} - \frac{\beta_{i3}\beta_{j3}}{\beta_{33}}.$$

The compliance coefficients can be expressed in terms of engineering constants as

$$\begin{aligned} \beta_{11} &= 1/E_1 \\ \beta_{22} &= 1/E_2 \\ \beta_{12} &= -\nu_{12}/E_1 = -\nu_{21}/E_2 \ , \\ \beta_{16} &= \eta_{12,1}/E_1 = \eta_{1,12}/G_{12} \\ \beta_{26} &= \eta_{12,2}/E_2 = \eta_{2,12}/G_{12} \\ \beta_{66} &= 1/G_{12} \quad , \end{aligned} \tag{5}$$

where E_k are the Young's moduli refering to the axes x_k, G_{12} is the shear modulus for the plane, ν_{ij} are Poisson's ratios and $\eta_{jk,l}$ and $\eta_{l,jk}$ are the mutual coefficients of first and second kind, respectively. For orthotropic materials $\beta_{16} = \beta_{26} = 0$. For plane stress problem in orthotropic materials one can write

$$\begin{bmatrix} \sigma_{11} \\ \sigma_{22} \\ \sigma_{12} \end{bmatrix} = \mathbf{D} \begin{bmatrix} \varepsilon_{11} \\ \varepsilon_{22} \\ 2\varepsilon_{12} \end{bmatrix} , \tag{6}$$

where

$$\mathbf{D} = \begin{bmatrix} E_1/e & E_2\nu_{12}/e & 0 \\ E_2\nu_{12}/e & E_2/e & 0 \\ 0 & 0 & G_{12} \end{bmatrix}$$

with $e = 1 - \frac{E_2}{E_1}(\nu_{12})^2$.

The following boundary and initial conditions are assumed

$u_i(\mathbf{x},t) = \tilde{u}_i(\mathbf{x},t)$on Γ_u

$t_i(\mathbf{x},t) = \tilde{t}_i(\mathbf{x},t)$ on Γ_t

$u_i(\mathbf{x},t)|_{t=0} = u_i(x,0)$ and $\dot{u}_i(\mathbf{x},t)|_{t=0} = \dot{u}_i(x,0)$ in Ω,

where Γ_u is the part of the global boundary with prescribed displacement and on Γ_t the traction vector is prescribed.

3 Local boundary integral equations in Laplace transform domain

Applying the Laplace transformation to the governing equation (1), we have

$$\overline{\sigma}_{ij,j}(\mathbf{x},p) - \rho p^2 \overline{u}_i(\mathbf{x},p) = -\overline{F}_i(\mathbf{x},p) \quad , \tag{7}$$

where

$$\overline{F}_i(\mathbf{x},p) = \overline{X}_i(\mathbf{x},p) + \rho p u_i(\mathbf{x},0) + \rho \dot{u}_i(\mathbf{x},0)$$

is the redefined body force in the Laplace transform domain with initial boundary condition for displacements $u_i(\mathbf{x},0)$ and velocities $\dot{u}_i(\mathbf{x},0)$.

The Laplace transform of function $f(\mathbf{x},t)$ is defined as

$$L[f(x,t)] = \overline{f}(x,p) = \int_0^\infty f(x,t)e^{-pt}d\tau,$$

where p is the Laplace transform parameter.

Instead of writing the global weak form for the above governing equation, the MLPG methods construct the weak form over local subdomains such as Ω_s, which is a small region taken for each node inside the global domain [Atluri and Shen (2002a); Zhu et al. (1998)]. The

local subdomains overlap each other, and cover the whole global domain Ω. The local subdomains could be of any geometric shape and size. In the current paper, the local subdomains are taken to be of circular shape. The local weak form of the governing equation (7) can be written as

$$\int_{\Omega_s} \left[\overline{\sigma}_{ij,j}(\mathbf{x},p) - \rho p^2 \overline{u}_i(\mathbf{x},p) + \overline{F}_i(\mathbf{x},p)\right] u_i^*(\mathbf{x})\, d\Omega = 0 \quad , \tag{8}$$

where $u_i^*(\mathbf{x})$ is a test function.

Using

$$\sigma_{ij,j}u_i^* = (\sigma_{ij}u_i^*)_{,j} - \sigma_{ij}u_{i,j}^*$$

and applying the Gauss divergence theorem one can write

$$\int_{\partial\Omega_s} \overline{\sigma}_{ij}(\mathbf{x},p) n_j(\mathbf{x}) u_i^*(\mathbf{x}) d\Gamma - \int_{\Omega_s} \overline{\sigma}_{ij}(\mathbf{x},p) u_{i,j}^*(\mathbf{x}) d\Omega + \int_{\Omega_s} \left[-\rho p^2 \overline{u}_i(\mathbf{x},p) + \overline{F}_i(\mathbf{x},p)\right] u_i^*(\mathbf{x}) d\Omega = 0, \tag{9}$$

where $\partial\Omega_s$ is the boundary of the local subdomain which consists of three parts $\partial\Omega_s = L_s \cup \Gamma_{st} \cup \Gamma_{su}$. L_s is the local boundary that is totally inside global domain, Γ_{st} is the part of the local boundary which coincides with the global traction boundary, i.e., $\Gamma_{st} = \partial\Omega_s \cap \Gamma_t$, and similarly Γ_{su} is the part of local boundary that coincides with the global displacement boundary, i.e., $\Gamma_{su} = \partial\Omega_s \cap \Gamma_u$.

If a Heaviside step function is chosen as the test function $u_i^*(\mathbf{x})$ in each subdomain

$$u_i^*(\mathbf{x}) = \begin{cases} 1 \ \text{at} \ \mathbf{x} \in \Omega_s \\ 0 \ \text{at} \ \mathbf{x} \notin \Omega_s \end{cases}$$

and considering

$$\overline{t}_i(\mathbf{x},p) = \overline{\sigma}_{ij}(\mathbf{x},p) n_j(\mathbf{x})$$

the local weak form (9) is leading to local boundary integral equations

$$\int_{\partial\Omega_s} \overline{t}_i(\mathbf{x},p) d\Gamma + \int_{\Omega_s} \left[-\rho p^2 \overline{u}_i(\mathbf{x},p) + \overline{F}_i(\mathbf{x},p)\right] d\Omega = 0 \quad . \tag{10}$$

Rearranging unknown terms on the left hand side we get

$$\int_{L_s} \overline{t}_i(\mathbf{x},p) d\Gamma + \int_{\Gamma_{su}} \overline{t}_i(\mathbf{x},p) d\Gamma - \int_{\Omega_s} \rho p^2 \overline{u}_i(\mathbf{x},p) d\Omega = -\int_{\Gamma_{st}} \tilde{\overline{t}}_i(\mathbf{x},p) d\Gamma - \int_{\Omega_s} \overline{F}_i(\mathbf{x},p) d\Omega. \tag{11}$$

Equation (11) is recognized as the overall force equilibrium on the subdomain Ω_s. In case of stationary problems the domain integral on the left hand side of this local boundary integral equation disappears. Then, a pure contour integral formulation is obtained under the assumption of vanishing body sources and homogeneous initial conditions.

In the MLPG method the test and trial function are not necessarily from the same functional spaces. For internal nodes, the test function is chosen as the Heaviside step function with support on the local subdomain. The trial function, on the other hand, is chosen to be the moving least squares (MLS) interpolation over a number of nodes randomly spread within the domain of influence. While the local subdomain is defined as the support of the test function on which the integration is carried out, the domain of influence is defined as a region where the weight function is not zero and all nodes lying inside are considered for interpolation. The approximated function can be written as [Atluri and Shen (2002a,b)]

$$\overline{\mathbf{u}}^h(\mathbf{x},p) = \mathbf{\Phi}^{\mathrm{T}}(\mathbf{x}) \cdot \hat{\mathbf{u}}(\mathrm{p}) = \sum_{\mathrm{a}=1}^{\mathrm{n}} \phi^{\mathrm{a}}(\mathbf{x}) \hat{\mathbf{u}}^{\mathrm{a}}(\mathrm{p}) \tag{12}$$

where the nodal values $\hat{\mathbf{u}}^a(p)$ are fictitious parameters and $\phi^a(\mathbf{x})$ is the shape function associated with the node a. The number of nodes, n, used for the approximation of $\overline{u}_i(\mathbf{x},p)$ is determined by the weight function $w^a(\mathbf{x})$. A 4^{th} order spline type weight function is considered in the present work

$$w^a(\mathbf{x}) = \begin{cases} 1 - 6\left(\frac{d^a}{r^a}\right)^2 + 8\left(\frac{d^a}{r^a}\right)^3 - 3\left(\frac{d^a}{r^a}\right)^4 & 0 \le d^a \le r^a \\ 0 & d^a \ge r^a \end{cases} , \tag{13}$$

where $d^a = \|\mathbf{x} - \mathbf{x}^a\|$ and r^a is the size of the support domain. It is seen that C^1 continuity is ensured over the

entire domain, therefore the continuity condition of tractions is satisfied.

The traction vectors $\bar{t}_i(\mathbf{x},p)$ at a boundary point $\mathbf{x}\in\partial\Omega_s$ are approximated in terms of the same nodal values $\hat{\mathbf{u}}^a(p)$ as

$$\bar{\mathbf{t}}^h(\mathbf{x},p)=\mathbf{N}(\mathbf{x})\mathbf{D}\sum_{a=1}^{n}\mathbf{B}^a(\mathbf{x})\hat{\mathbf{u}}^a(p) \tag{14}$$

where the matrix **N(x)** is related to the normal vector **n(x)** on $\partial\Omega_s$ by

$$\mathbf{N}(\mathbf{x})=\begin{bmatrix} n_1 & 0 & n_2 \\ 0 & n_2 & n_1 \end{bmatrix}$$

and the matrix $\mathbf{B}^a$ is represented by the gradients of the shape functions as

$$\mathbf{B}^a=\begin{bmatrix} \phi^a_{,1} & 0 \\ 0 & \phi^a_{,2} \\ \phi^a_{,2} & \phi^a_{,1} \end{bmatrix} \quad .$$

Obeying the boundary conditions at those nodal points on the global boundary, where displacements are prescribed, and making use of the approximation formulae (12), one obtains the discretized form of the displacement boundary conditions given as

$$\sum_{a=1}^{n}\phi^a(\zeta)\hat{\mathbf{u}}^a(p)=\tilde{\bar{\mathbf{u}}}(\zeta,p)\ \text{ for }\ \zeta\in\Gamma_u. \tag{15}$$

Furthermore, in view of the MLS-approximation (12) and (14) for unknown fields in the local boundary integral equations (11), we obtain the discretized LIE

$$\begin{aligned}
&\sum_{a=1}^{n}\hat{\mathbf{u}}^a(p)\int_{L_s}\mathbf{N}(\mathbf{x})\mathbf{D}\mathbf{B}^a(\mathbf{x})d\Gamma \\
&+\sum_{a=1}^{n}\hat{\mathbf{u}}^a(p)\int_{\Gamma_{su}}\mathbf{N}(\mathbf{x})\mathbf{D}\mathbf{B}^a(\mathbf{x})d\Gamma \\
&-\rho p^2\sum_{a=1}^{n}\hat{\mathbf{u}}^a(p)\int_{\Omega_s}\phi^a(\mathbf{x})d\Omega \\
&=-\int_{\Gamma_{st}}\tilde{\bar{\mathbf{t}}}(\mathbf{x},p)d\Gamma-\int_{\Omega_s}\overline{\mathbf{F}}(\mathbf{x},p)d\Omega
\end{aligned} \tag{16}$$

which are considered on the sub-domains adjacent to interior nodes as well as to the boundary nodes on Γ_{st}.

Collecting the discretized LIE together with the discretized boundary conditions for displacements, we get the complete system of algebraic equations for computation of nodal unknowns which are the Laplace transforms of fictitious parameters $\hat{\mathbf{u}}^a(p)$.

The time dependent values of the transformed variables can be obtained by an inverse transform. There are many inversion methods available for the Laplace transformation. As the Laplace transform inversion is an ill-posed problem, small truncation errors can be greatly magnified in the inversion process and lead to poor numerical results. In the present analysis the Stehfest algorithm [Stehfest (1970)] is used. An approximate value f_a of the inverse $f(t)$ for a specific time t is given by

$$f_a(t)=\frac{\ln 2}{t}\sum_{i=1}^{N}v_i\,\overline{f}\left(\frac{\ln 2}{t}i\right) \quad , \tag{17}$$

where

$$v_i=(-1)^{N/2+i}\sum_{k=[(i+1)/2]}^{\min(i,N/2)}\frac{k^{N/2}(2k)!}{(N/2-k)!\,k!\,(k-1)!\,(i-k)!\,(2k-i)!} \quad . \tag{18}$$

The selected number $N=10$ with a single precision arithmetic is optimal to receive accurate results. It means that for each time t, it is needed to solve N boundary value problems for the corresponding Laplace parameters $p=i\ln 2/t$, with $i=1,2,...,N$. If M denotes the number of the time instants in which we are interested to know $f(t)$, the number of the Laplace transform solutions $\overline{f}(p_j)$ is then $M\times N$.

4 Time dependent Local boundary integral equations

The local weak form of the governing equation (1) can be written as

$$\int_{\Omega_s}\left[\sigma_{ij,j}(\mathbf{x},t)-\rho\ddot{u}_i(\mathbf{x},t)+X_i(\mathbf{x},t)\right]u_i^*(\mathbf{x})\,d\Omega=0 \quad . \tag{19}$$

Applying the Gauss divergence theorem to the first inte-

gral one obtains

$$\int_{\partial\Omega_s} \sigma_{ij}(\mathbf{x},t)n_j(\mathbf{x})u_i^*(\mathbf{x})d\Gamma - \int_{\Omega_s} \sigma_{ij}(\mathbf{x},t)u_{i,j}^*(\mathbf{x})d\Omega + \int_{\Omega_s} \left[-\rho\ddot{u}_i(\mathbf{x},t)+X_i(\mathbf{x},t)\right]u_i^*(\mathbf{x})d\Omega = 0 \quad . \tag{20}$$

If we will use the same test function as in the Laplace transform approach, the local boundary integral equation (LBIE) has the form

$$\int_{L_s} t_i(\mathbf{x},t)d\Gamma + \int_{\Gamma_{su}} t_i(\mathbf{x},t)d\Gamma - \int_{\Omega_s} \rho\ddot{u}_i(\mathbf{x},t)d\Omega = -\int_{\Gamma_{st}} \tilde{t}_i(\mathbf{x},t)d\Gamma - \int_{\Omega_s} X_i(\mathbf{x},t)d\Omega. \tag{21}$$

Substituting the MLS approximations for displacements (12) and tractions (14) into (20), we get the set of discretized LBIEs

$$\sum_{a=1}^{n} \hat{\mathbf{u}}^a(t)\int_{L_s} \mathbf{N}(\mathbf{x})\mathbf{D}\mathbf{B}^a(\mathbf{x})d\Gamma + \sum_{a=1}^{n} \hat{\mathbf{u}}^a(t)\int_{\Gamma_{su}} \mathbf{N}(\mathbf{x})\mathbf{D}\mathbf{B}^a(\mathbf{x})d\Gamma - \rho\sum_{a=1}^{n} \hat{\ddot{\mathbf{u}}}^a(t)\int_{\Omega_s} \phi^a(\mathbf{x})d\Omega = -\int_{\Gamma_{st}} \tilde{\mathbf{t}}(\mathbf{x},t)d\Gamma - \int_{\Omega_s} \mathbf{X}(\mathbf{x},t)d\Omega \tag{22}$$

considered at nodal points $\mathbf{x} \notin \Gamma_u$. The discretized displacement boundary conditions

$$\sum_{a=1}^{n} \phi^a(\zeta)\hat{\mathbf{u}}^a(t) = \tilde{\mathbf{u}}(\zeta,t) \tag{23}$$

are considered at nodal points $\zeta \in \Gamma_u$.

Depending on the boundary conditions, the system of ordinary differential equations (21) - (22) can be rearranged in such a way that all known quantities are on the r.h.s. Thus, in matrix form the system becomes

$$\mathbf{L}\ddot{\mathbf{x}} + \mathbf{K}\mathbf{x} = \mathbf{P} \quad . \tag{24}$$

There are many time integration procedures for the solution of this system of ordinary differential equations. In the present work the Houbolt method is applied. In the Houbolt finite difference scheme [Houbolt (1950)] the acceleration ($\ddot{\mathbf{u}} = \ddot{\mathbf{x}}$) is expressed as

$$\ddot{\mathbf{x}}_{\tau+\Delta\tau} = \frac{2\mathbf{x}_{\tau+\Delta\tau} - 5\mathbf{x}_{\tau} + 4\mathbf{x}_{\tau-\Delta\tau} - \mathbf{x}_{\tau-2\Delta\tau}}{\Delta\tau^2} \quad , \tag{25}$$

where $\Delta\tau$ is the time step.

Substituting eq. (24) into eq. (23), we get the system of algebraic equations for the unknowns $\mathbf{x}_{\tau+\Delta\tau}$:

$$\left[\frac{2}{\Delta\tau^2}\mathbf{L} + \mathbf{K}\right] x_{\tau+\Delta\tau} = \mathbf{L}\frac{1}{\Delta\tau^2}\left\{5\mathbf{x}_{\tau} - 4\mathbf{x}_{\tau-\Delta\tau} + \mathbf{x}_{\tau-2\Delta\tau}\right\} + \mathbf{P} \tag{26}$$

The value of the time step has to be appropriately selected with respect to material parameters (propagation velocities) and time dependence of the boundary conditions.

5 Numerical examples

In this section numerical results will be presented to illustrate the implementation and effectiveness of the proposed method. In the first example, a thin circular orthotropic disc is rotating around x_3 axis perpendicular to the plane of disc. For such a case analytical solution is available [Lekhnickii (1963)]. The stress components depend only on the radial coordinate r :

$$\sigma_r = \frac{1}{2}\rho\omega^2 R^2(1-A)\left[1-(r/R)^2\right]$$

$$\sigma_\varphi = \frac{1}{2}\rho\omega^2 R^2\left\{(1-A)\left[1-(r/R)^2\right] + 2A\,(r/R)^2\right\}$$

$$\sigma_{r\varphi} = 0$$

$$A = \frac{\beta_{11}+2\beta_{12}+\beta_{22}}{3\beta_{11}+2\beta_{12}+\beta_{66}+3\beta_{22}}, \tag{27}$$

where R is the radius of the disc, ω is angular freguency and the constant A is an invariant with the transformation of the coordinate system. The same problem was analyzed by Zhang et al. (1997) by the boundary element method. We have used the same material constants as in the mentioned work. They correspond to glass-epoxy composite: $E_1 = 48.26\,GPa$, $E_2 = 17.24\,GPa$, $G_{12} = 6.89\,GPa$, $\nu_{12} = 0.29$. The body forces due the rotation are

$$X_1 = \rho x_1 \omega^2$$

$X_2 = \rho x_2 \omega^2$.

Since the constant A is an invariant with transformation of the coordinate system, for simplicity, the material principal axes are also taken as x_1 and x_2 here. Due to the symmetry with respect to x_1 and x_2 axes, only the first quarter of the disc is numerically modelled. For MLS approximations we have used totally 99 nodes with 37 of them were located on global boundary of analyzed domain. The radius of the disc is

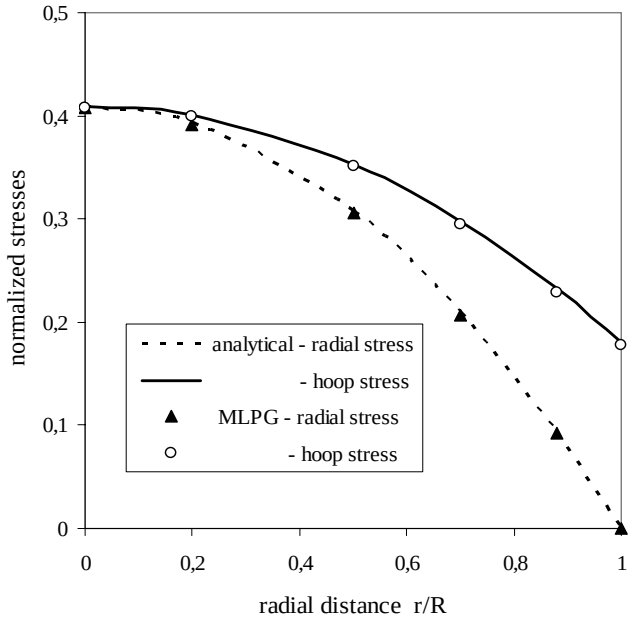

Figure 1 : Variation of radial and hoop stresses with radial coordinate in the rotating disc

considered to be $R = 1$. The radius of circular subdomains is selected as $r_{loc} = 0.05$. Results of radial and hoop stresses, normalized by $\rho\omega^2 R^2$, are compared with the analytical solution in Figure 1. One can observe excellent agreement between two sets of results on the whole radial interval. The Sobolev norm of the stress errors

$$r_s = \frac{\|\sigma^{num} - \sigma^{exact}\|}{\|\sigma^{exact}\|} \times 100\% \text{with } \|\sigma\| = \left(\int_\Omega \sigma \sigma^d \Omega \right)^{1/2}$$

is 0,7%. The variation of normalized displacements with radial coordinate is shown in Fig. 2. Results are normalized by $\rho\omega^2 R^3 / E_2$. Displacements in x_2 direction significantly exceed those in

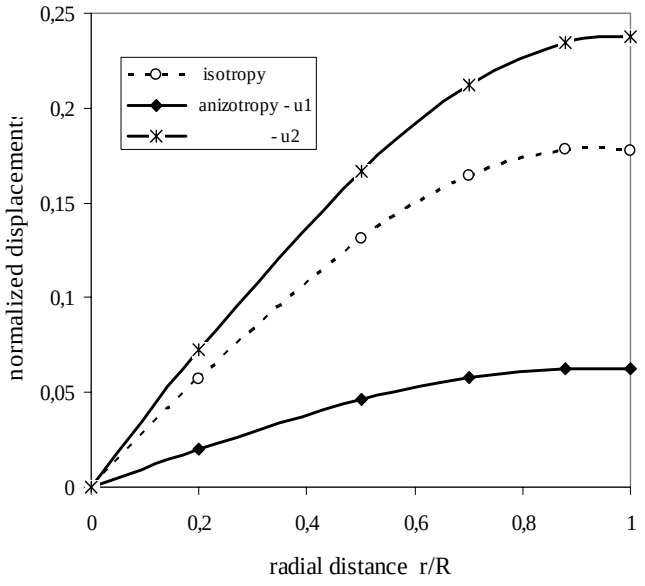

Figure 2 : Variation of displacements with radial coordinate in the rotating disc

perpendicular direction since $E_1 > E_2$. Presented numerical results for isotropic case correspond to $E_1 = E_2 = 17.24 GPa, \nu = 0.29$.

In the second numerical example an anisotropic bar with material constants, $E_1 = 1.31 \cdot 10^5 MPa$, $E_2 = 0.13 \cdot 10^5 MPa$, $G_{12} = 0.064 \cdot 10^5 MPa$, $\nu_{12} = 0.038$ and $\rho = 10$ is fixed at the upper end. The bar is loaded only by its own weight. Plane strain conditions are assumed for a square cross section with the side length equal to $a = 1$. Analytical solution for normal stress and displacement components in the direction of the weight are given as

$$\sigma_{22}(x_2) = \rho g x_2$$

$$u_2(x_2) = \frac{1}{2} \rho g \tilde{\beta}_{22} (x_2)^2 \quad .$$

A regular node distribution with 32 nodes is used for numerical solution. Displacements and stresses are normalized by $\rho g \tilde{\beta}_{22}$ and $\rho g a$, respectively. Variations of both normalized quantities are presented in Figures 3 and 4. Excellent agreement of numerical results with analytical solution is observed for displacements and stresses.

In the third numerical example natural frequencies for a simple orthotropic structure are computed. A beam with length $a = 2m$ and width $b = 0.5m$ is fixed at both ends with shorted sides. The following material properties are considered: $E_1 = 1 \cdot 10^{11} Pa$, $E_2 = 2 \cdot 10^{11} Pa$,

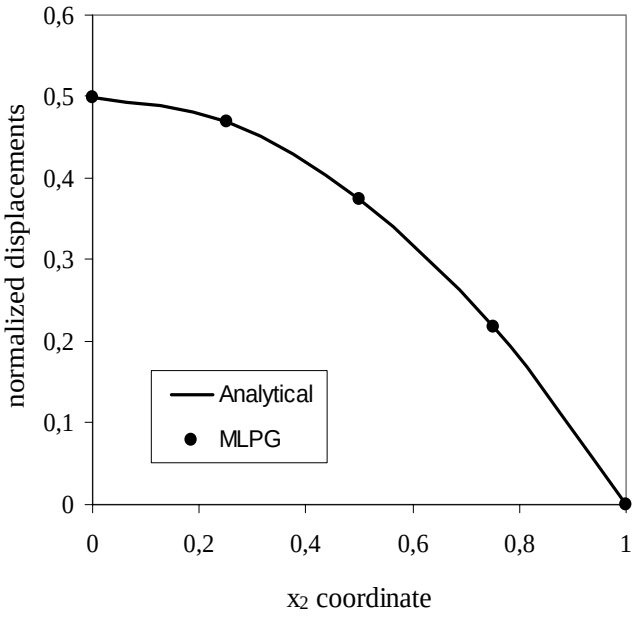

Figure 3 : Variation of normalized displacements with X2 coordinate in the bar under own weight

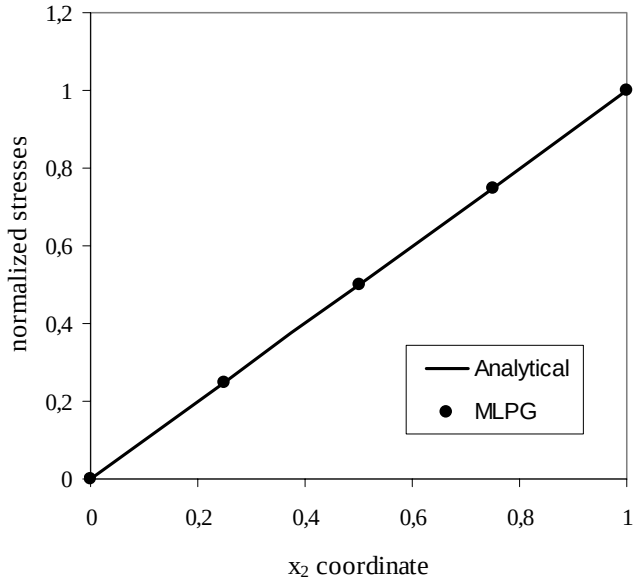

Figure 4 : Variation of normalized stresses σ_{22} with x_2 coordinate in the bar under own Weight

$G_{12} = 0.769 \cdot 10^{11} Pa$, $\nu_{12} = 0.3$ and $\rho = 8000 kg/m^3$. Plane stress conditions are assumed. The same problem was analyzed by Albuquerque et al. (2002). A regular node distribution with 120 nodes is used for numerical solution. We have compared our results with those obtained by NASTRAN code (FEM analysis) where a fine mesh with 400 quadrilateral elements was used. Relative errors of LBIE with respect to NASTRAN results for natural frequencies are given in Table 1. In the first five natural frequencies, the relative error is less than 1%.

Table 1 : Natural frequencies of bi-fixed beam

LBIE	NASTRAN	Relative error [%]
382	383.87	0.49
885	890.63	0.63
889	892.91	0.44
1482	1492.77	0.72
1759	1772.66	0.77

In the fourth numerical example, we analyze a long strip subjected to prescribed traction vector with Heaviside time dependence, $t_1 = 10H(t-0)$ at the end $x_1 = L$, and the opposite end is fixed in x_1-direction, (Figure 5).

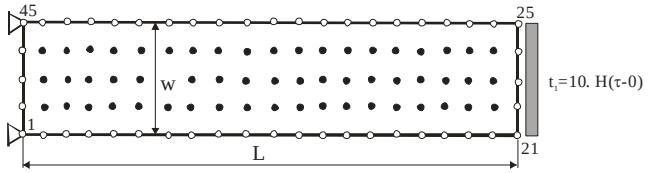

Figure 5 : Long Orthotropic strip under a uniaxial tension

The other boundaries are free of tractions. The length of the strip is $L = 10$ and the width $w = 2$. Firstly, the isotropic strip is analyzed with the following material properties: $E = 10^4$, Poisson ratio $\nu = 0.2$ and the mass density $\rho = 1$. The numerical results obtained by the present LBIE method in the Laplace transformed domain are compared with the conventional BEM results. In the LBIE method 48 boundary nodes and additional 57 internal nodes with a regular distribution is used for numerical modeling. Time variation of the displacement component u_1 at the mid of the strip, $x_1 = L/2$, is shown in Figure 6.

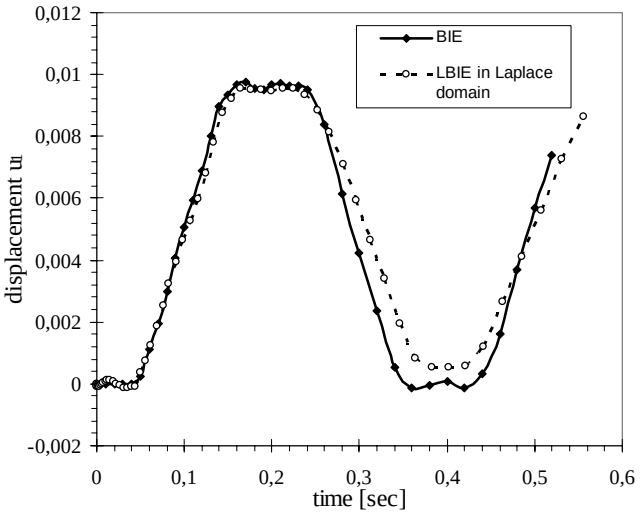

Figure 6 : Time variation of displacement component u_1 at the middle of the isotropic strip

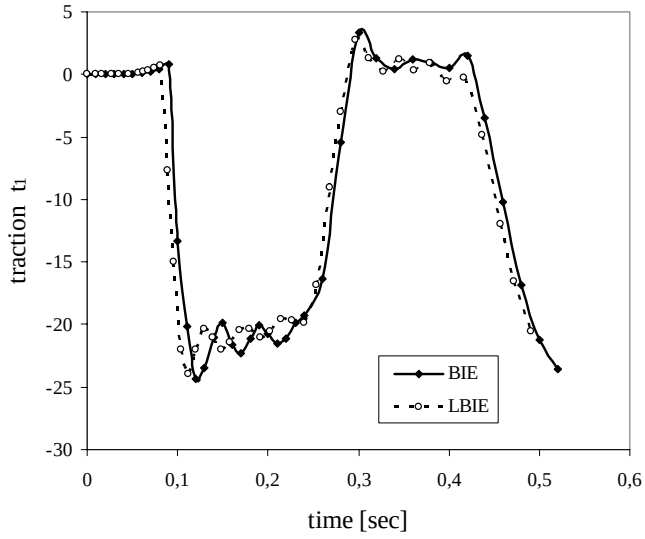

Figure 7 : Time variation of the traction vector at the fixed end of the isotropic strip

One can observe a quite good agreement of both present results. The time variation of the traction vector at the fixed end, $x_1 = 0$, is shown in Figure 7.

Now, an orthotropic strip with the same geometry is analyzed. The following material properties are considered: $E_1 = 2 \cdot 10^4$, $E_2 = 10^4$, $G_{12} = 0.416 \cdot 10^4$, $\nu_{12} = 0.2$ and $\rho = 1$. It means that all material parameters are the same like in isotropic case except E_1 and we introduce

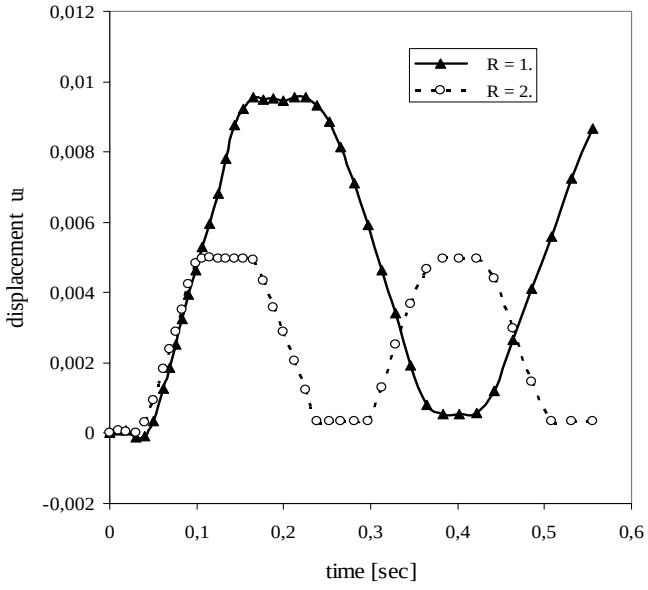

Figure 8 : Influence of the Young's moduli ratio in orthotropic strip on time variation of the displacement component

parameter $R = E_1/E_2 = 2$. With increasing R the velocity of propagation waves in x_1 is enhanced and maximum value of displacements is reduced for larger value of Young modulus. Time variations of displacements and tractions for orthotropic strip are given in Figures 8 and 9, respectively. In orthotropic strip higher frequency of picks of displacements and tractions is observed than in the isotropic counterpart.

In the last numerical example a rectangular orthotropic plate with a central crack is analyzed. Plate is loaded by a uniform static load as is shown in Figure 10.

The following geometry is considered: $w = 1$, $a/w = 0.5$, $h = w$. To test the proposed method an isotropic material properties are considered: $E = 10^4$, Poisson ratio $\nu = 0.25$. A regular node distribution with 400 and 900 nodes is used for numerical solutions, respectively. Relative errors with respect to Murakami's handbook results are given in Table 1. For a gradually changing node distribution at crack tip vicinity the number of nodes for numerical modeling is expected to be smaller at the same accuracy as for regular node distribution. Regular node distribution is selected here only to simplify input data.

Rather hypothetical orthotropic material is used next to have a possibility to compare results with Bowie and

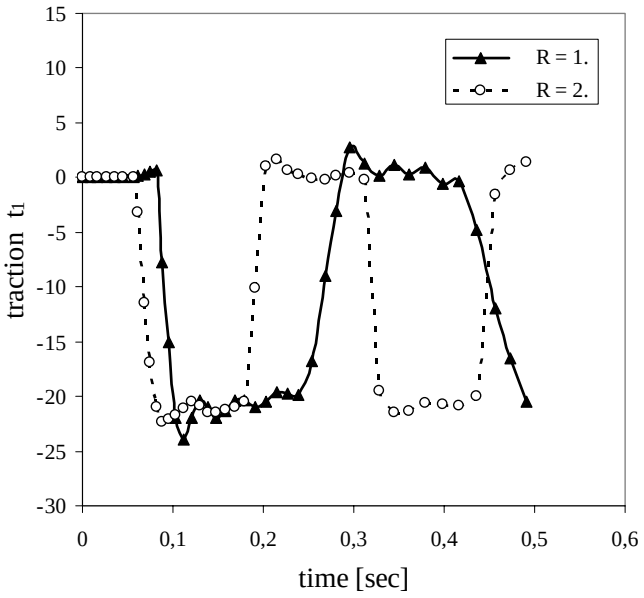

Figure 9 : Influence of the Young's moduli ratio in orthotropic strip on time variation of the traction vector

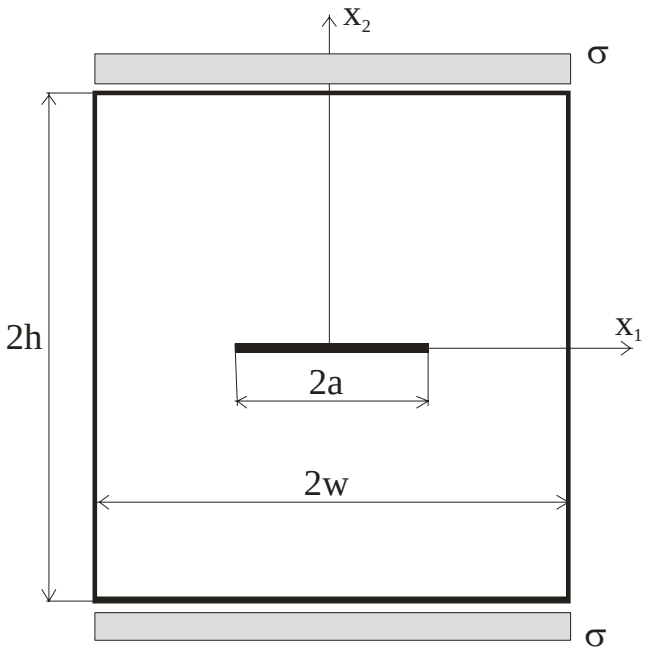

Figure 10 : Rectangular orthotropic plate with a central crack

Freeze (1972). These material properties are chosen such that the roots of the characteristic equation are purely imaginary and one of them with the imaginary part equal to unity. The shear modulus G_{12} and Poisson's ratio ν_{12} were fixed and the Young's moduli were evaluated as a function of the parameter $R = E_1/E_2$ with $E_1 = G_{12}(R + 2\nu_{12} + 1)$, $E_2 = E_1/R$, $G_{12} = 6GPa$, $\nu_{12} = 0.03$. Five various ratios were considered, $R = 0.1$, 0.5, 0.9, 2.5, 4.5. The stress intensity factor is computed from the asymptotic expansion of displacements at the crack tip vicinity. In a pure I mode crack opening one can write for displacements on crack surface

$$u_2 = 2\sqrt{\frac{2r}{\pi}} D_{21} K_I$$

where r is a radial distance of the evaluation point from the crack tip, K_I is the stress intensity factor and

$$D_{21} = Im\left\{\frac{\mu_2 P_{21} - \mu_1 P_{22}}{\mu_1 - \mu_2}\right\}$$

$$P_{ik} = \begin{bmatrix} \beta_{11}\mu_k^2 + \beta_{12} - \beta_{16}\mu_k \\ \beta_{12}\mu_k + \beta_{22}/\mu_k - \beta_{26} \end{bmatrix},$$

and μ_k are rots of characteristic equation

$$\beta_{11}\mu^4 - 2\beta_{16}\mu^3 + (2\beta_{12} + \beta_{66})\mu^2 - 2\beta_{26}\mu + \beta_{22} = 0 \quad .$$

Results for normalized stress intensity factor, $f_I = K_I/\sigma\sqrt{\pi a}$ for various R are given in Figure 11. The present results show good agreement with Bowie and Freeze (1972). Percentage error is less than 1,5%.

Table 2 : Normalized stress intensity factors

Sources		Stress intensity factor f_I	Relative errors [%]
Murakami´s Handbook		1.32	-
LBIE	400 nodes	1.290	2.27
	900 nodes	1,309	0,8

6 Conclusions

- A local boundary integral equation formulation based on MLPG in Laplace transform-and time-domain with meshless approximation has been successfully implemented to solve 2-d initial-boundary value problems for static and elastodynamic problems in anisotropic solids.

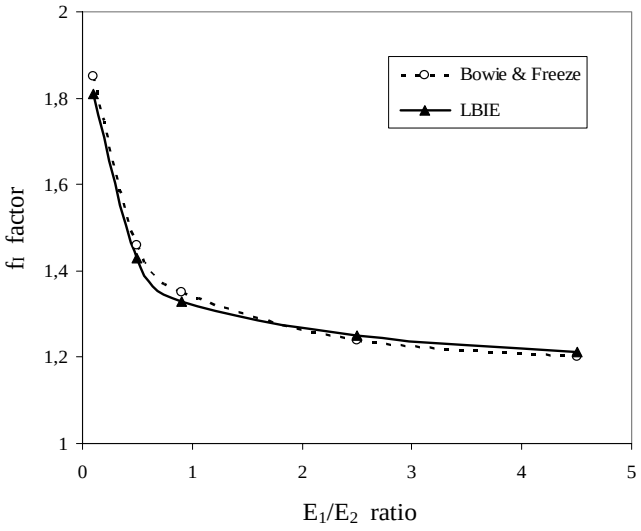

Figure 11 : Variation of normalized stress intensity factor with Young's moduli ratio

- The Heaviside step function is used as test function in the local symmetric weak form. The derived local boundary-domain integral equations are non-singular. The analyzed domain is divided into small overlapping circular sub-domains on which the local boundary integral equations are applied. The proposed method is truly meshless methods, wherein no elements or background cells are involved in either the interpolation or the integration.

- The proposed method yields a pure contour integral method for stationary boundary conditions even for nonhomogeneous material properties. An extension of the proposed method to continuously nonhomogeneous anisotropic bodies is expected in the near future.

- The main drawback of the boundary element anisotropic formulations is the absence of well-established fundamental solutions in elastodynamic.The proposed method is leading to a simple integral formulation and can be easily generalized to continuously nonhomogeneous solids. The computational accuracy of the present method is comparable with that of FEM. However, the efficiency and the adaptability of the present method is higher than in the conventional FEM because of eliminating the mesh generation troubles.

Acknowledgement: The authors acknowledge the support by the Slovak Science and Technology Assistance Agency registered under number APVT-51-003702, as well as by the Slovak Grant Agency VEGA – 2303823.

References

Albuquerque, E. L.; Sollero, P.; Aliabadi, M. H. (2002a): The boundary element method applied to time dependent problems in anisotropic materials. *International Journal Solids and Structures*, 39: 1405-1422.

Albuquerque, E. L.; Sollero, P.; Fedelinski, P. (2002b): Boundary element method applied to modal analysis of anisotropic structures, in: *Boundary Element Techniques (eds. Z. Yao, M.H. Aliabadi)*, Springer, 65-70.

Ang, W. T. ; Telles, J. C. F. (2004): A numerical Green's function for multiple cracks in anisotropic bodies, *Journal of Engineering Mathematics*, 49: 197-207.

Atluri, S. N. (2004): *The Meshless Local Petrov-Galerkin Method for Domain & BIE Discretizations*, 680 pages, Tech Science Press.

Atluri, S. N.; Shen, S. (2002a): *The Meshless Local Petrov-Galerkin (MLPG) Method*, Tech Science Press.

Atluri, S. N.; Shen, S. (2002b): The meshless local Petrov-Galerkin (MLPG) method: A simple & less-costly alternative to the finite element and boundary element method, *CMES: Computer Modeling in Engineering & Sciences*, 3: 11-51.

Atluri, S. N.; Sladek, J.; Sladek, V.; Zhu, T. (2000): The local boundary integral equation (LBIE) and its meshless implementation for linear elasticity. *Comput. Mech.*, 25: 180-198.

Atluri, S. N.; Han, Z. D.; Shen, S. (2003): Meshless local Petrov-Galerkin (MLPG) approaches for solving the weakly-singular traction & displacement boundary integral equations. *CMES: Computer Modeling in Engineering & Sciences*, 4: 507-516.

Belytschko, T.; Lu, Y.; Gu, L. (1994): Element free Galerkin methods. *Int. J. Num. Meth. Engn.*, 37: 229-256.

Belytschko, T.; Krogauz, Y.; Organ, D.; Fleming, M.; Krysl, P. (1996): Meshless methods; an overview and recent developments. *Comp. Meth. Appl. Mech. Engn.*, 139: 3-47.

Bowie, O. L.; Freeze, C. E. (1972): Central crack in

plane orthotropic rectangular sheet. *International Journal of Fracture* 8: 49-58.

Clements, D. L.; Haselgrove, M. D. (1983): A boundary integral equation method for a class of crack problems in anisotropic elasticity, *International Journal of Comput. Math.,* 12: 267-278.

Cole, D. M.; Kosloff, D.; Minster, J. B. (1978): A numerical boundary integral method for elastodynamics. *Bulletin of the Seismological Society in America*, 68: 1331-1357.

Cruse, T. A.; Swedlow, J. L. (1971): *Interactive Program for Analysis and Design Problems in Advanced Composistes Technology*. Carnegie-Mellon University Report AFML-TR-71-268.

Ding, H.; Liang, J.; Chen, B. (1997): The unit point force solution for both isotropic and transversaly isotropic media. *Communications in Numerical Methods in Engineering*, 13: 95-102.

Dominguez, J. (1993): *Boundary Elements in Dynamics*, Computational Mechanics Publications.

Dumir, P. C.; Mehta, A. K. (1987): Boundary element solution for elastostatic orthotropic half-plane problems. *Computer & Structures* 26: 431-438.

Eshelby, J. D; Read, W. T.; Shockley, W. (1953): Anisotropic elasticity with applications to dislocations. *Acta Metallurgica*, 1: 251-259.

Houbolt, J. C. (1950): A recurrence matrix solution for the dynamic response of elastic aircraft. *Journal of Aeronautical Sciences*, 17: 371-376.

Kogl, M.; Gaul, L. (2000): A 3-D boundary element method for dynamic analysis of anisotropic elastic solids. *CMES: Computer Modeling in Engineering & Sciences*, 1: 27-43.

Lekhnitskii, S. G. (1963): *Theory of Elasticity of an Anisotropic Body*, Holden Day.

Manolis, G. D.; Beskos, D. E. (1988): *Boundary Element Methods in Elastodynamics*, Unwin Hyman.

Mikhailov, S. E. (2002): Localized boundary-domain integral formulations for problems with variable coefficients. *Engn. Analysis with Boundary Elements*, 26: 681-690.

Murakami, Y. (1987): *Stress Intensity Factor Handbook*, Pergamon Press.

Nardini, D.; Brebbia, C. A. (1983): A new approach to free vibration analysis using boundary elements. *Applied Mathematical Modelling*, 7: 157-162.

Pan, E.; Amadei, B. (1996): Fracture mechanics analysis of cracked 2-d anisotropic media with a new formulation of the boundary element method. *International Journal of Fracture* 64: 161-174.

Pan, E.; Amadei, B.; Kim, Y. I. (1998): 2-D BEM analysis of anisotropic half-plane problems – application to rock mechanics. *International Journal of Rock Mechanics and Mining Science & Beomechanics Abstracts*, 35: 195-218.

Pan, E. (1999): A BEM analysis of fracture mechanics in 2d anisotropic piezoelectric solids. *Engineering Analysis with Boundary Elements,* 23: 67-76.

Perez-Gavilan, J. J.; Aliabadi, M. H. (2000): A Galerkin boundary element formulation with dual reciprocity for elastodynamics. *International Journal for Numerical Methods in Engineering,* 48: 1331-1344.

Schanz, M.; Antes, H. (1997): Application of Operational Quadrature Methods in time domain boundary element methods. *Meccanica*, 32: 179-186.

Schclar, S. N. (1994): *Anisotropic Analysis Using Boundary Elements*, Computational Mechanics Publications.

Sladek, V.; Sladek, J. (1983): Transient elastodynamic three-dimensional problems in cracked bodies. *Applied Mathematical Modelling*, 8: 2-10.

Sladek, J.; Sladek, V.; Atluri, S. N. (2000): Local boundary integral equation (LBIE) method for solving problems of elasticity with nonhomogeneous material properties. *Computational Mechanics,* 24: 456-462.

Sladek, J.; Sladek, V.; Van Keer, R. (2003a): Meshless local boundary integral equation method for 2D elastodynamic problems. *Int. J. Num. Meth. Engn*., 57: 235-249

Sladek, J.; Sladek, V.; Zhang, Ch. (2003b): Application of meshless local Petrov-Galerkin (MLPG) method to elastodynamic problems in continuously nonhomogeneous solids, *CMES: Computer Modeling in Engineering & Sciences*, 4: 637-648.

Snyder, M. D.; Cruse, T. A. (1975): Boundary integral analysis of anisotropic cracked plates. *International Journal of Fracture* 31: 315-328.

Sollero, P.; Aliabadi M. H. (1993): Fracture mechanics analysis of anisotropic plates by the boundary element method. *International Journal of Fracture* 64: 269-284.

Sollero, P.; Aliabadi, M. H. (1993): Anisotropic analysis ofcracks in composite laminates by the boundary element method. *Composite Structures* 31, 229-233.

Stehfest, H. (1970): Algorithm 368: numerical inversion of Laplace transform. *Comm. Assoc. Comput. Mach*., 13: 47-49.

Wang, C. Y.; Achenbach, J. D. (1996): Two dimensional time domain BEM for scattering of elastic waves in solids of general anisotropy. *International Journal of Solids and Structures*, 33: 3843-3864.

Zhang, J. J.; Tan, C. L.; Afagh, F. F. (1997): Treatment of body-force volume integrals in BEM by exact transformation for 2-D anisotropic elasticity. *International Journal for Numerical Methods in Engineering,* 40: 89-109.

Zhu, T.; Zhang, J. D.; Atluri, S. N. (1998): A local boundary integral equation (LBIE) method in computational mechanics, and a meshless discretization approach. *Computational Mechanics,* 21: 223-235.